Local and Macroscopic Thermal Transport from a Sphere in a Turbulent Air Stream

T. R. GALLOWAY and B. H. SAGE

Chemical Engineering Laboratory
California Institute of Technology, Pasadena, California 91109

The local and macroscopic thermal transport from a calorimeter-instrumented sphere 1.5 in. in diameter located in an air stream was measured experimentally in the subcritical flow regime. The Reynolds number was varied between 5,200 and 70,200 with artificially induced turbulence level varying from 0.013 to 0.256. Higher turbulence increased thermal transport through the laminar boundary layer prevailing in the forward hemisphere, and significantly retarded the point of separation from about 87° to 106° as measured from stagnation. An increase in the Reynolds number shifted the point of separation forward and altered the behavior in the wake. In the separated wake region, the experimental evidence indicated that the vortex reattached to the rear surface and formed a new boundary layer that resulted in a decrease in the local thermal transfer.

There has been a significant number of investigations of the macroscopic transport from spheres into turbulent air streams. Only limited investigations are available of the local thermal transport from spheres (*1* to *3*) when the free stream turbulence is systematically varied. The phenomenon of the effects of free stream turbulence on heat and mass transfer from bluff bodies has been reviewed by Kestin (*4*) with the conclusions that the localized augmentation in a laminar boundary layer is real and significant. The alteration of the outer flow velocity profile from wake effects is the result of free stream turbulence. The recent experimental background has been summarized (*5*, *6*) by regression analysis of the available experimental data and the results expressed in analytical form. The so-called "Frössling Group" *Fs* has been employed as an effective means of describing the macroscopic and local thermal transport as a function of Reynolds number and level of turbulence.

ANALYTICAL CONSIDERATIONS

A recent summary by Evans (*7*) covers the various current mathematical techniques for solving the Navier-Stokes and energy equations in the laminar boundary layer on bluff bodies. The greatest emphasis is on cylinders, although material is presented on spheres and other shapes. The best theoretical technique applicable in the vicinity of the forward stagnation point is shown to be that of Merk (*7*). Such behavior was also found in this study. The accuracy of the prediction depends strongly on the applicability of the expression describing the velocity profile. It turns out that the transport is directly dependent upon the coefficient of the leading term in the outer flow expansion. For example, for air ($Pr = 0.7$) the Frössling Group becomes:

$$Fs = 0.5299\,[2A]^{1/2} \tag{1}$$

where

$$\frac{v_1}{v_\infty} = A\left(\frac{X}{D}\right) + \cdots$$

This expression is applicable for a laminar forward stagnation point. For inviscid flow, A is equal to three. For real fluids the coefficient is always less than three and owing to the phenomenon of separation is dependent upon Reynolds number, free stream turbulence, wake blockage effects, and the like. Comparisons will be made between Equation (1) using various outer flow expressions presented in the literature and the current experimental measurements.

Few expressions are available analogous to Equation (1) that are applicable to a forward stagnation point subjected to flow at an elevated free stream turbulence. This problem is the subject of another effort (*8*), which derives a theoretical expression covering a wide range of Prandtl numbers and turbulence levels. It is, however, the purpose of this work to present an experimental study on the localized effects of free stream turbulence on the thermal transfer from spheres to assist in the resolution of some of the less well understood aspects of the phenomenon as has been recently summarized by Kestin (*4*), and to check the accurcay of prediction of the empirical expressions derived earlier (*5*, *6*).

Numerous experimental factors require that the terms employed be defined with care (*9*). The Reynolds number is based on the character of the free stream.

$$Re_x = U_x d/\nu_\infty \tag{2}$$

In the foregoing equation, the molecular properties of the fluid stream at a distance from the sphere have been employed to describe the transport. The Frössling number was defined in two ways as is indicated in the following expressions for spheres involving thermal and material transfer, respectively:

$$Fs_\infty = \frac{Nu_\infty - 2}{Re_\infty^{1/2}\, Pr_{m,\infty}^{1/3}} \tag{3}$$

$$Fs_\infty = \frac{Sh_\infty - 2}{Re_\infty^{1/2}\, Sc_{m,\infty}^{1/3}} \tag{4}$$

The molecular properties of the free stream at a distance from the sphere have been employed to describe such transport phenomena. The Frössling number in the laminar boundary layer has been shown (*8*, *9*) to be nearly a linear function of the square root of the Reynolds number

T. R. Galloway is with Shell Development Company, Emeryville, California 94608.

TABLE 1. PROPERTIES OF DRY AIR AT ATMOSPHERIC PRESSURE

Property	Units	Temperature, °F. 70	100	130
Isobaric heat capacity (*12-14*)	B.t.u./(lb.) (°F.)	0.2403	0.2405	0.2407
Kinematic viscosity × 10^4 (*12, 13*)	sq. ft./sec.	1.63	1.80	1.97
Molecular Prandtl number (*12, 13*)		0.710	0.705	0.703
Specific volume (*10-12*)	cu. ft./lb.	13.35	14.11	14.86
Thermal conductivity × 10^6 (*12, 13*)	B.t.u./(sec. ft.) (°F.)	4.14	4.34	4.54
Thermometric conductivity × 10^4 (*12, 13*)	sq. ft./sec.	2.30	2.54	2.80
Viscosity × 10^7 (*12, 13*)	(lb.) (sec.)/sq. ft.	3.82	3.98	4.14

with the level of turbulence being treated as a parametric variable. The molecular properties of the air stream employed in the resolution of the experimental results to be described are set forth in Table 1. The basic references (*10* to *14*) employed for each of the several quantities are included in a part of Table 1.

EXPERIMENTAL METHODS

Arrangement of the air supply to the free jet and the details of the turbulence grid and the approach section are shown in Figure 1, together with the general location of the calorimeter-instrumented sphere. The speed of the blower was controlled by means of a quartz crystal (*15*) which maintained the speed of the blower within 0.2% or 5° angular rotation, whichever is the larger measure of uncertainty. The temperature of the air stream approaching the turbulence grid was maintained within 0.1°F. of 100°F. This temperature was established by means of a strain free, platinum resistance thermometer which had been calibrated against a similar instrument standardized by the National Bureau of Standards. The temperature of the air stream was known relative to the international platinum scale within 0.15°F.

The velocity distribution of a section through the jet passing through the axis of the sphere is shown for two Reynolds numbers in Figure 2. The jet emerging from the 6-in. by 6-in. extension shown in Figure 1 yielded a velocity that was independent of the position in the jet throughout a region approximately 4 in. by 4 in. The sphere was located on the axis of the 6-in. by 6-in. extension.

The total flow was measured by means of Herschel-type venturi meters (*16*) used in conjunction with a kerosene-air manometer. The difference in elevation of the kerosene was determined by means of a cathetometer, and appropriate corrections (*17, 18*) were made to the calibration of the venturi meter for the effects of Reynolds number.

In this investigation, measurements were not taken if the Reynolds number, measured by using the dimensions of the throat section of the venturi meter, was lower than 10,000. Under such condition the calibration factor was 0.9645. At higher Reynolds numbers this calibration factor gradually approached unity.

Two sectional views of the instrumented sphere are shown in Figure 3. Essentially the sphere consists of two mated parts which could be rotated with respect to one another by means of the gear assembly "A" which is actuated through the stem "B". Furthermore, the entire sphere may be rotated about the hollow stem "C". Such an arragnement permitted the calorimeter shown at "D" to be located over a large portion of the surface of the sphere relative to stagnation. A heater was provided at "E" and was wound in a groove cut in the copper cylinder "F" and filled with epoxy adhesive. The cylinder "F" was remachined and another copper cylinder was shrunk over the heater. This outside surface fitted snugly into the two mated portions of the sphere. All moving copper surfaces were plated with 0.0002 in. hard chrome. Experimental measurements at high Reynolds numbers with the calorimeter in the upstream portion of the sphere indicated that the maximum variation in surface temperature as determined by means of the thermocouples "G" and "H" was 0.4°F., which is significantly smaller than that experienced with the smaller silver spheres used earlier (*2, 3*).

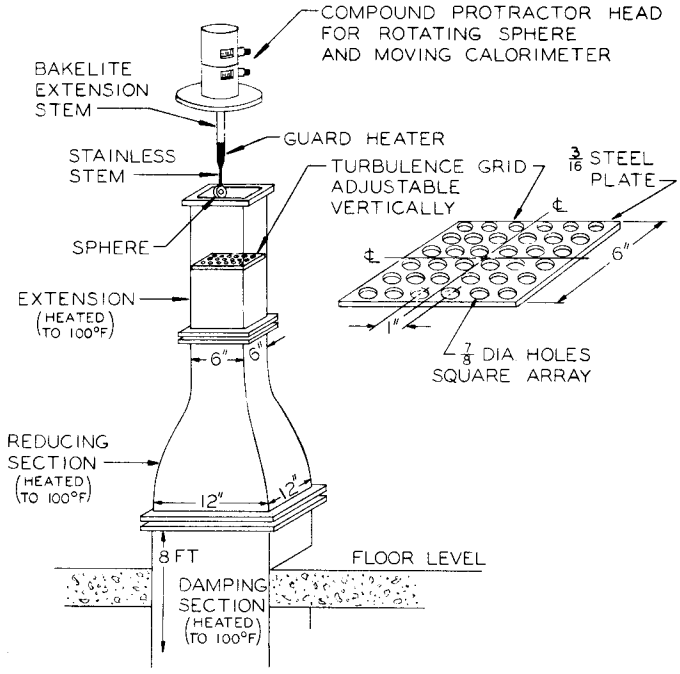

Fig. 1. Arrangement of free jet air supply.

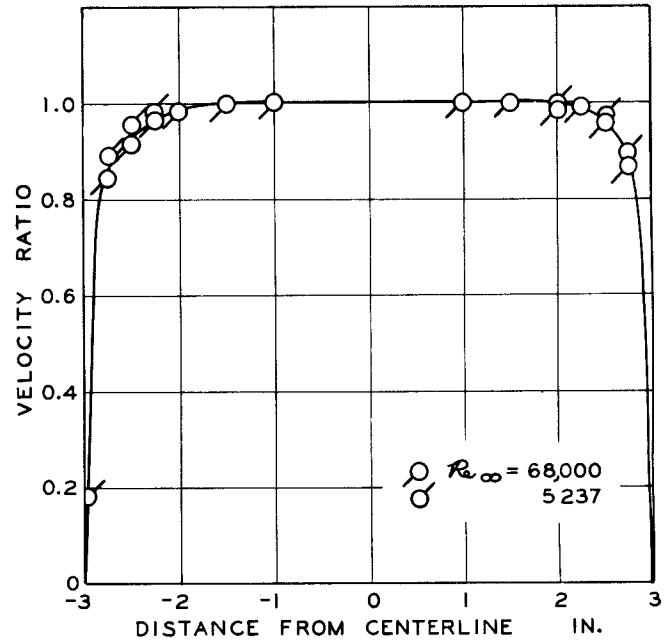

Fig. 2. Velocity profile across the 6 × 6 in. free jet.

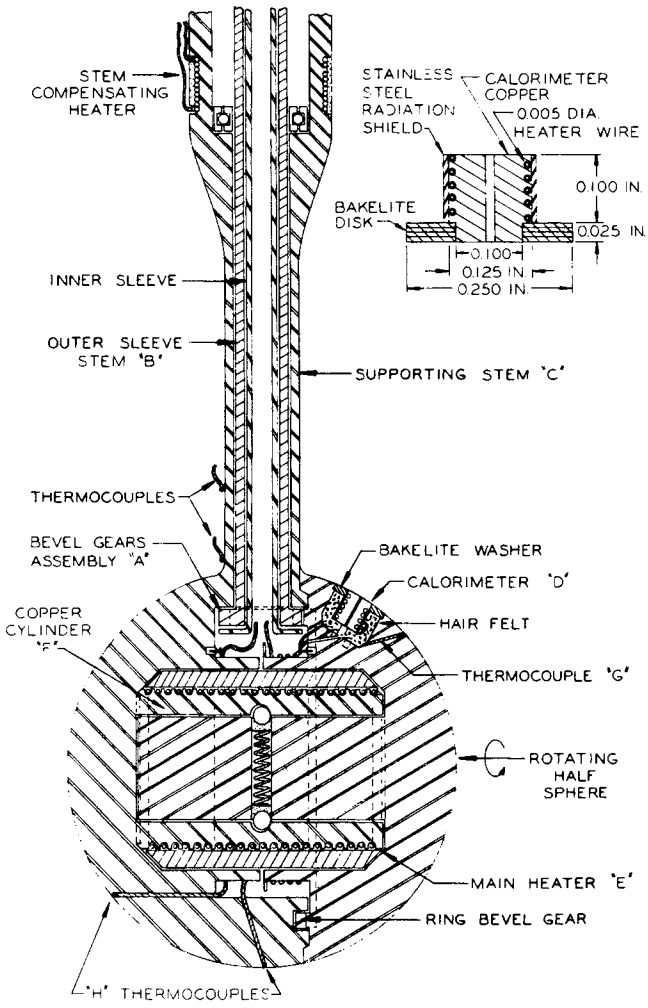

Fig. 3. Details of instrumented sphere.

The details of the calorimeter "D" are shown in an insert to Figure 3. It was provided with a small internal wire-wound heater enclosed in a radiation shield. Plastic insulation was provided between the body of the sphere and the calorimeter section itself. Some uncertainty exists as a result of the surface roughness and temperature of this annular insulation but when it is considered that the entire area of the insert is only 2.91% of the total area of the sphere, the opportunity for boundary layer growth while the stream was crossing the insulation was small relative to the total growth on the sphere. In operation, the temperature of the calorimeter surface was maintained within 0.01°F. of the temperature of the adjacent portions of the sphere. The active area of the calorimeter was only 0.466% of the area of the sphere and permitted good resolution of the local transport. A guard heater was provided within the hollow stem "C" that decreased the thermal conduction from the sphere along the stem to a negligible value.

The Nusselt number of the sphere as a whole was established from

$$Nu_\infty^* = 9.02175 \frac{I^2R - (I^2R)_0}{K_\infty \, \Delta T} \qquad (4)$$

where $(I^2R)_0$ is the thermal loss at no flow. The surface area of the sphere 1.467 in. in diameter available for thermal transfer, corrected for the stem area and effective calorimeter area, was 0.04622 sq. ft. The molecular thermal conductivity of the free stream K was employed to establish the Nusselt number. Thermocouples in the calorimeter were calibrated over the temperature range involved with a strain-free, platinum resistance thermometer described earlier. It is believed that the thermocouples yielded values of the surface temperature within 0.15°F. relative to the international platinum scale. There was no difficulty in obtaining the equality of temperature between the calorimeter and the adjacent spherical surface and at two points along the stem of the instrumented sphere within 0.01°F. The experimental reproducibility in the overall Nusselt number was 0.9%.

The local Nusselt number was calculated without need to obtain an effective calorimeter area for thermal transfer. Laboratory measurements at each angle were made of the current applied to the calorimeter heater which was just sufficient to raise its temperature to that of the surrounding spherical surface. The resistance of the heaters could be measured accurately while briefly interrupting the current using a four-wire lead system and a Mueller bridge circuit (9). These measurements were made with no air flow but with all components of the sphere and working section duct walls heated as required. This energy dissipation as a function of temperature driving force and angle from stagnation $[i(\psi)^2R]_0$ was used to correct for radiation and free convection losses. With air flowing the temperatures throughout the installation were carefully controlled and the balancing current measured at each position of the calorimeter. The following relation was then used to compute the local Nusselt number directly from the local calorimeter current, the surface area average calorimeter current, and the simultaneously measured current in the main heater for the sphere.

$$Nu_\infty = \frac{i(\psi)^2 r - [i(\psi)^2 r]_0}{1/2 \int_0^{180°} \{i(\psi)^2 r - [i(\psi)^2 r]_0\} \, d(\cos\psi)} Nu_\infty^* \qquad (5)$$

This procedure requires that the local Nusselt number, when integrated over the spherical surface, will be equal to the more accurately determined overall Nusselt number.

EXPERIMENTAL RESULTS

The experimental results are recorded in Table 2 and list the polar angle and its cosine, along with the associated conditions of flow for each of the ten sets of test conditions investigated. The temperature difference between the

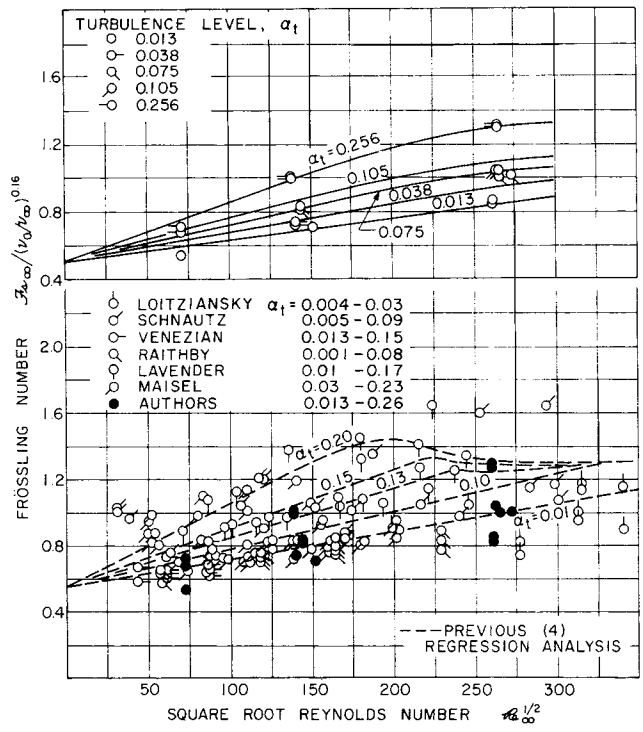

Fig. 4. Effect of Reynolds number upon the macroscopic Frössling number.

TABLE 2. EXPERIMENTAL RESULTS FOR LOCAL AND MACROSCOPIC TRANSPORT FROM THE 1.5-IN. SPHERE

		Test	654	655	656	657	658
		Nu°	34.308	45.59	122.59	105.41	92.39
		Re_∞	5,237.6	5,237.8	19,266.9	20,886.2	19,967.9
		Z_t	0.013	0.256	0.256	0.075	0.038
		Fs°	0.5326	0.7077	0.9925	0.8196	0.7348
Polar angle	Cos ψ	ν_∞/ν_0	0.9836	0.9877	0.9881	0.9863	0.9847
36.87	0.8	$Fs =$	—	1.0391	1.3595	1.1525	1.1261
45.57	0.7		0.8718	1.0269	1.3109	1.1045	1.0600
53.13	0.6		0.8614	—	1.2861	1.0567	1.0138
60.00	0.5		0.7750	1.0323	1.2448	0.9906	0.9534
66.42	0.4		0.7508	—	1.1865	0.9364	0.8891
72.54	0.3		—	0.8767	1.1189	0.8441	0.7765
78.46	0.2		0.5906	—	1.0402	0.7073	0.6277
84.26	0.1		—	0.6938	0.9230	0.5323	0.4617
90.00	0.0		0.3526	0.5997	0.7892	0.4132	0.3539
95.74	−0.1		0.2876	0.4608	0.6793	0.4188	0.3871
101.54	−0.2		0.2972	0.4022	0.6640	0.5348	0.4404
107.46	−0.3		0.3368	0.4054	0.7660	0.6359	0.4725
113.58	−0.4		0.3464	0.4548	0.8952	0.7048	0.530
120.00	−0.5		0.3457	0.4820	0.9219	0.7033	0.5554
126.87	−0.6		0.3426	0.4815	0.8597	0.6793	0.5422
134.43	−0.7		0.3338	0.4648	0.7666	0.7191	0.5758
143.13	−0.8		0.3451	0.5439	0.7525	0.8562	0.7236
150.00	−0.86602		0.3587	0.6618	0.8435	0.9908	0.8949

		Test	659	660	661	662	663
		Nu°	95.16	197.30	238.07	241.59	302.06
		Re_∞	22,953.8	67,788.7	70,240.4	69,872.7	69,939.4
		Z_t	0.013	0.013	0.075	0.105	0.256
		Fs°	0.7058	0.8513	1.0094	1.0270	1.2835
Polar angle	Cos ψ	ν_∞/ν_0	0.9843	0.9841	0.9865	0.9879	0.9911
36.87	0.8	$Fs =$	1.1020	1.1554	1.2285	1.3109	1.5320
45.87	0.7		1.0470	1.1386	1.1873	1.2595	1.5028
53.13	0.6		0.9956	1.0971	1.1270	1.2137	—
60.00	0.5		0.9446	1.0210	1.0861	1.1625	1.4420
66.42	0.4		0.8891	0.8940	1.0351	1.1218	—
72.54	0.3		0.7771	0.7474	0.9778	1.0576	1.3321
78.46	0.2		0.6245	0.5401	0.9110	0.9928	—
84.26	0.1		0.4664	0.4955	0.7914	0.9003	1.2012
90.00	0.0		0.3418	0.4858	0.6577	0.7594	1.1296
95.74	−0.1		0.3748	0.5238	0.5546	0.6283	1.0620
101.54	−0.2		0.4606	0.5597	0.6163	0.6078	1.0323
107.46	−0.3		0.4978	0.6569	1.0003	0.8104	1.0780
113.58	−0.4		0.4981	0.7312	1.2124	1.1175	1.2458
120.00	−0.5		0.4762	0.7981	1.2285	1.1961	1.3464
126.87	−0.6		0.4694	0.8164	1.1178	1.0933	1.2972
134.43	−0.7		0.5142	0.8597	1.0005	0.9409	1.2082
143.13	−0.8		0.6428	0.9911	0.9407	0.8233	1.0569
150.00	−0.86602		0.7857	1.1426	1.0011	0.8653	1.1163

sphere and air stream was 10°F. The level of turbulence in the wake of the grid was estimated from the measurements of Davis (*19, 20*). These are considered only apparent levels of turbulence since the authors (*19, 20*) reported them as longitudinal turbulence levels. It has been assumed in the present instance involving nonuniform flow that the turbulence was isotropic. The integral scale of turbulence was expected (*9*) to vary from 0.3 to 0.6 in. The velocity distribution across the central portion of the jet was uniform as indicated in Figure 2 except in the case of investigations involving an apparent level of turbulence of 0.256, where measurable variations in average velocity across the working section were encountered as a result of the proximity of the sphere to the grid shown on the insert in Figure 1.

The effect of the Reynolds number upon the overall macroscopic Frössling number is shown in Figure 4. The standard error of estimate of the experimental points from a smooth curve drawn through them for a level of turbulence of 0.013 is 4.9%, and for all the points from their corresponding smooth curves the standard error of estimate was 2.1%. Such deviations from smooth curves exceed the experimental reproducibility of 0.9% and suggest that further improvements could be made in control of the thermal conditions at the surface of the sphere. It was more difficult to hold steady conditions at the lower Reynolds numbers. Therefore, the smooth curves are believed to describe quantitatively the effects of Reynolds number and free stream turbulence level on the Frössling number within 2%.

As a matter of interest, other experimental values for macroscopic Frössling numbers are presented in the lower part of Figure 4. The current data are in good agreement with the values reported by Loitziansky (*21, 22*), Venezian (*3*), and Raithby (*23*), all for turbulence levels below 0.04. The experimental results from the several authors

diverge as the turbulence level increases up to 0.23. The dashed curves represent nonlinear multiple regression analysis (5) of results of a large number of authors involving 947 data points. In addition to the measurements examined earlier (5) the results of Schnautz (24) for mass transfer, Lavender and Pei (25) for heat transfer, and Raithby and Eckert (23) for mass transfer have been included.

The scatter present in the work of Schnautz (24) is large and only qualitative trends with turbulence are apparent. Lavender and Pei's results (25), using the perforated plate turbulence grid, show clearly the effects of turbulence level, but the presence of vortices downstream from their cross-flow stem, 90° from stagnation and not guard heated, appear to have increased the overall transport by approximately 20%. Raithby and Eckert (23) studied the influence of cross-flow versus rear support stems and found the overall transport to be enhanced by nearly 10% when cross flow stems were used as compared with rear-supported spheres provided with guard heaters. These transport studies (23), covering turbulence levels from 0.00155 to 0.07, are nearly identical to the results of this study.

The results of Venezian (3) compare closely with the current work especially when the estimation of the turbulence decay with distance from the grid is considered in detail. The measurements of Maisel and Sherwood (26) show large increases in transport with increases in free stream turbulence, and are in reasonable agreement with the results of the present work. The largest discrepancies seem to arise from differences in the detailed nature of the turbulence associated with the flow.

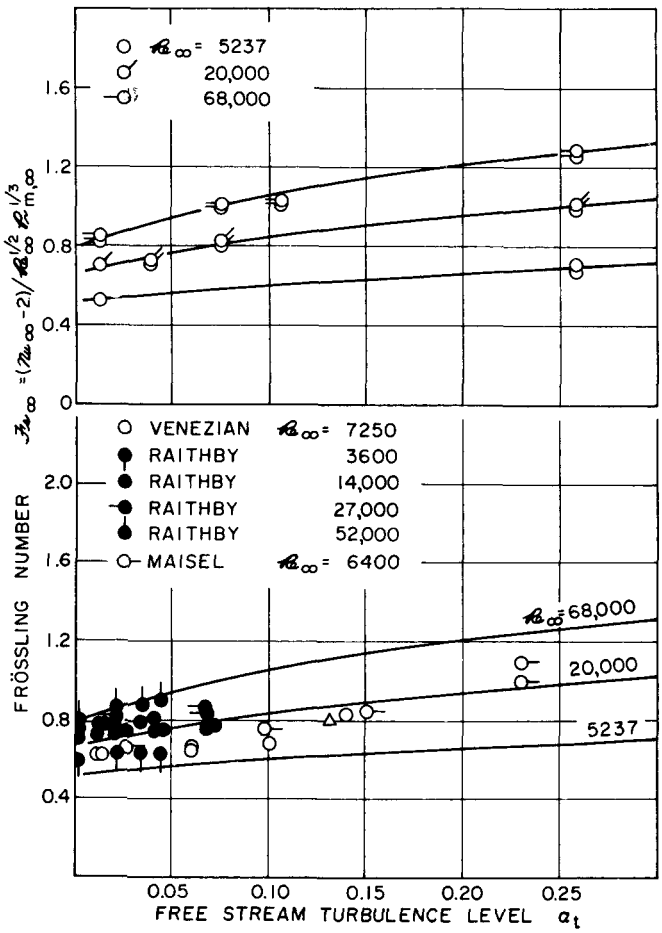

Fig. 5. Effect of turbulence level on the Frössling number.

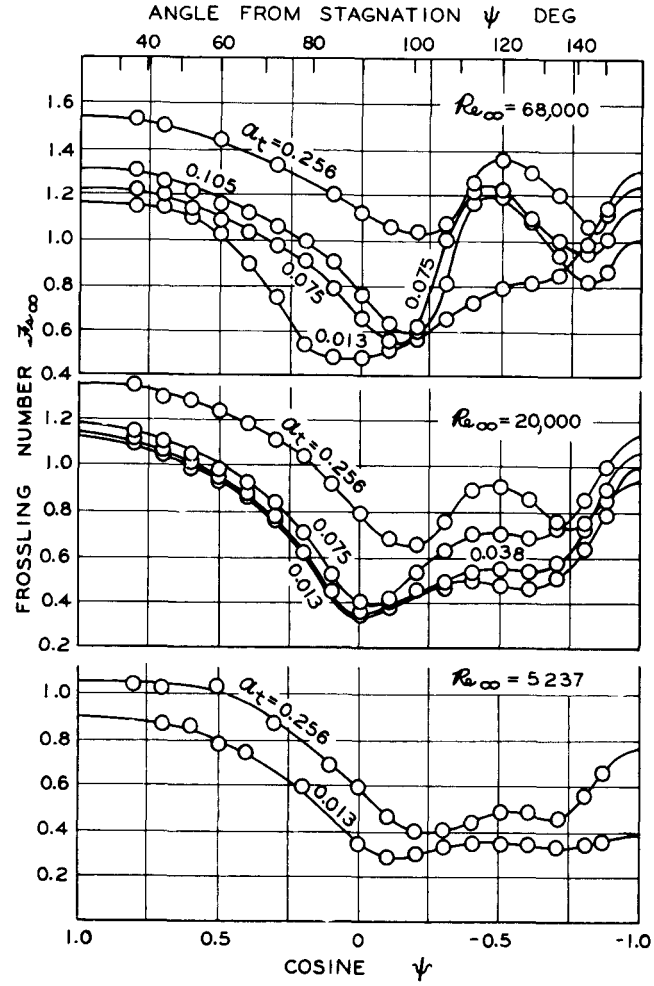

Fig. 6. Local transport from the 1.5-in. sphere at several Reynolds numbers.

The effect of free stream turbulence for three different values of Reynolds numbers covered in the present investigation is presented in Figure 5. The relation between Frössling number and turbulence level is nearly linear. The standard error of estimate of the experimental points from the smooth curve drawn through them was 2.1%. A comparison with other data concerning the effect of turbulence upon macroscopic thermal transport from spheres is presented in the lower part of Figure 5. Reasonable agreement with the earlier measurements of Maisel and Sherwood (26), Venezian (3), and Raithby and Eckert (23) was obtained. If the same data for estimating turbulence level were used for each set of data some of the bias between investigators would be reduced.

The local Frössling number is presented as a function of the polar angle from stagnation in Figure 6. The marked influence of the level of turbulence is evident. The Frössling number is substantially increased in the laminar boundary layer near the forward stagnation point with increases in turbulence level. Also, increases in the level of turbulence increase the locus of separation from a polar angle of approximately 87° for a level of turbulence of 0.013 to as much as 106° for a level of turbulence of 0.256 for a Reynolds number of 68,500. At this large Reynolds number and turbulence level, the laminar boundary layer formed at the forward stagnation point develops into a turbulent layer before the locus of separation is reached (5). Such a situation results in prolonging attachment. At $\alpha_t = 0.075$ this is apparent at $Re = 68{,}000$ but not at $Re = 20{,}000$.

Such a transition into supercritical flow not only alters the local transport behavior starting near 85° and delays separation but alters the magnitude of wake flow transport as well. At a slightly lower turbulence level of 0.105 the flow is probably trans-critical (5) and the transport near separation is reduced to the limit observed at lower turbulence levels. This large difference in the magnitude of the Frössling number near separation appears to be related to increased fluctuations in the separation locus over a larger portion of the sphere surface (9). Such an averaging mechanism tends to blend regions of low and high transport. A similar situation is observed at a Reynolds number of 20,000, comparing local transport for turbulence levels of 0.256 and 0.075. The separation of a turbulent boundary flow instead of a laminar boundary flow may be the source of such fluctuations.

The prominent maximum in the Frössling number in the region of wake flow, near 120° from stagnation, may well arise from a secondary stagnation locus formed by two coupled vortices. Judging from the increase in the maxima as the Reynolds number is increased the circulation pattern within the vortex must increase significantly at the higher Reynolds numbers. The small maxima at 180° may result from an aft stagnation point associated with the vortex formation.

The complicated behavior in the wake of the sphere, as suggested by earlier measurements (2, 3) involving the surface temperature gradients in the gas stream, has been confirmed by the information set forth in Figure 6. Similar information is presented in Figure 7 except that the effect of Reynolds number on the local transport at low and high turbulence levels is shown in the two parts of the diagram. As a result of the opposing effects of Reynolds number and turbulence level which nearly compensate each other, there is little change in the locus of separation with an increase in the Reynolds number from 5,200 to 68,000. At the low

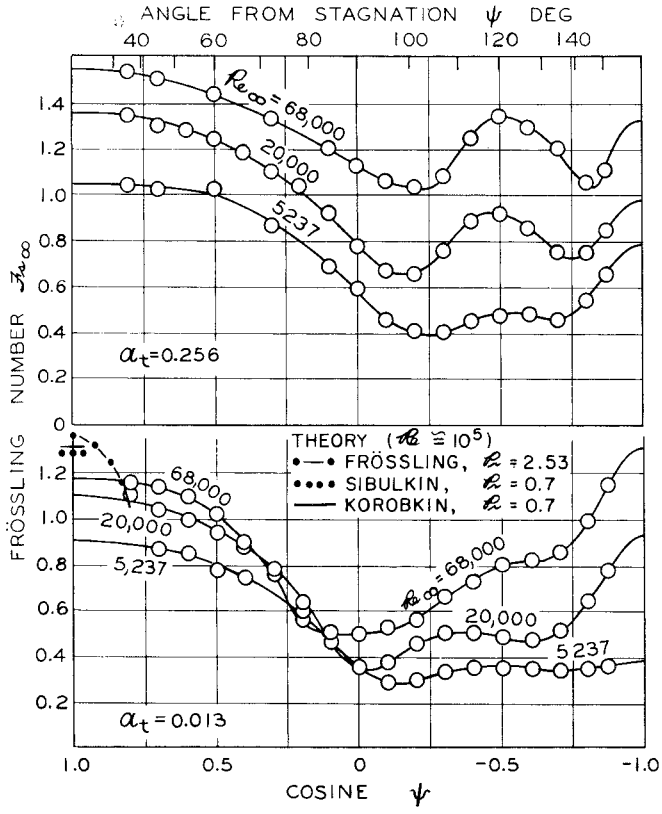

Fig. 7. Local transport from the 1.5-in. sphere at low and high turbulence.

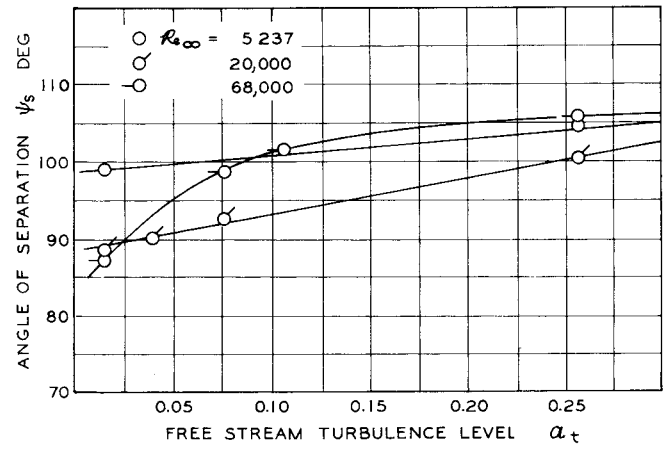

Fig. 8. The migration of the locus of separation.

turbulence levels, the effect of Reynolds number has overshadowed the effect of turbulence, and there is a corresponding decrease in the polar angle from stagnation to the locus of separation with an increase in Reynolds number. Furthermore, at 80° from the forward stagnation, near the locus of separation, there is substantially no effect of the Reynolds number upon the local Frössling number.

Figure 7 also illustrates that the thermal transport through the laminar boundary layer near the forward stagnation point depends more strongly on Reynolds number than the normal square root linear relationship. Such effect of Reynolds number was found earlier (6) and it is believed to arise from the alteration of the outer flow velocity profile with increasing wake length as a result of changing the Reynolds number. The well-known theoretical results for stagnation flow heat transfer by Korobkin (28) and Sibulkin (29) and for transport away from stagnation by Frössling (30) are shown in Figure 7 for comparison. The velocity distributions used in their calculations were all for Reynolds numbers considerably above those of the present study. Korobkin used the Tomotika experimental velocity distribution for $Re \cong 200{,}000$, Sibulkin assumed potential flow, and Frössling used the Page experimental velocity distribution for $Re = 157{,}000$ and obtained results for a Prandtl number of 2.53. When the latter is corrected (8) to a Prandtl number of 0.7 it matches the limit of Sibulkin. All of these theoretical predictions are for much higher Reynolds numbers than the measurements of this work. Good agreement is obtained with theory when this experimental work is extrapolated to Reynolds numbers between 157,000 and 200,000. As discussed, the effect of Reynolds number arises from the alteration of the wake flow which in turn alters the outer flow velocity distribution near the forward stagnation. The wake flow transport at high Reynolds numbers and turbulence levels in Figure 7 suggests supercritical flow phenomena resulting in a fluctuating separation locus as discussed earlier. These effects are almost identical to those observed for cylinders (27).

In Figure 8 is presented the effect of free-stream turbulence and Reynolds number upon the locus of separation, insofar as can be directly established from the current experimental measurements. It is apparent that at moderate Reynolds numbers there is a rapid, nearly linear increase in the angle of separation measured from stagnation as the free stream turbulence level is increased. At the higher Reynolds number there is a more rapid increase in the angle from the forward stagnation point to the locus of separation with increasing free-stream turbulence upon the approach to supercritical flow. These trends are similar to those found for cylinders (27).

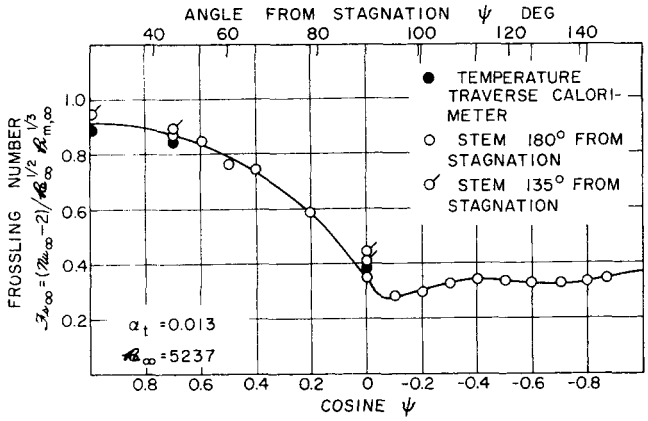

Fig. 9. Comparison of local transport using temperature traverse and calorimetric measurements.

There is shown in Figure 9 a comparison of the present data utilizing the calorimeter-instrumented sphere with data obtained by determining the temperature gradient at the surface of the 1.5-in. sphere. The agreement over a range of angles from stagnation of 0°, 45°, and 90° is considered satisfactory. The standard error of estimate of the data from the smooth curves utilizing the 15 calorimeter measurements was 1% and using the three temperature traverses was 2.5%. Such standard errors are considered a reasonable measure of agreement considering the widely different technique employed in arriving at the local values. With the sphere mounted at 45° such that the supporting stem emerged from the sphere surface at 135° from the forward stagnation point, the calorimeter indicated a local Frössling number 3.5% greater than previously established. Such behavior corroborates the findings of Raithby and Eckert (*23*).

ACKNOWLEDGMENT

The assistance of George Griffith in constructing the sphere, Henry Smith in the experimental work, a Virginia Berry in the review of the calculations associated with the resolution of these experimental measurements is acknowledged. Donna Johnson assisted in the preparation of the manuscript.

NOTATION

d = sphere diameter, ft.
h = heat transfer coefficient, B.t.u./(sec.)(sq.ft.)(°F.)
i = current applied to calorimeter heater, amperes
I = current applied to sphere main heater, amperes
K_x = thermal conductivity, B.t.u./(sec.)(ft.)(°F.)
Fs_∞ = Frössling number, $Nu_\infty/(Re_\infty^{1/2}\ Pr_{m,\infty}^{1/3})$
Nu_x = Nusselt number, $h_x d/K_x$
$Pr_{m,\infty}$ = Prandtl number, α_∞/ν_∞
r = electrical resistance of calorimeter heater, OHMS
R = electrical resistance of sphere main heater, OHMS
Re_x = Reynolds number, $U_x d/\nu_x$
$Sc_{m,\infty}$ = Schmidt number
Sh = Sherwood number
U_x = free-stream velocity, ft./sec.
u'_{zf} = longitudinal fluctuating velocity, ft./sec.

Greek Letters

α_∞ = thermal diffusivity, sq.ft./sec.
α_t = level of longitudinal turbulence, fraction $[(u'_{zf})^2]^{1/2}/U_x$
ΔT = temperature difference between sphere surface and free stream, °F.
ν_x = kinematic viscosity, sq.ft./sec.
ψ = angle measured streamwise from forward stagnation point, °

Subscripts

0 = denotes condition of no flow
∞ = denotes quantity evaluated using free stream properties

Superscript

* = denotes macroscopic value, describing total transport as opposed to local without asterisk

LITERATURE CITED

1. Wadsworth, J., *Nat. Res. Council Can., Div. Mech. Eng.* Report MT-39 (1958).
2. Short, W. W., R. A. S. Brown, and B. H. Sage, *J. Appl. Mech.*, **27**, 393 (1960).
3. Venezian, E., M. J. Crespo, and B. H. Sage, *AIChE. J.*, **8**, 383 (1962).
4. "Advances in Heat Transfer," Vol. 3, T. F. Irvine, Ed. Academic Press, New York (1966).
5. Galloway, T. R., and B. H. Sage, *Int. J. Heat Mass Transfer*, **10**, 1195 (1967).
6. *Ibid.*, **11**, 539 (1968).
7. Evans, H. L., "Laminar Boundary-Layer Theory," Addison-Wesley, Reading, Mass. (1968).
8. Galloway, T. R., submitted to A.S.M.E., *J. Heat Transfer.*
9. Galloway, T. R., Ph.D. dissertation, Calif. Inst. Tech., Pasadena (1967).
10. "International Critical Tables," 3, 3 (1928).
11. Stops, D. W., *Nature*, **164**, 966 (1949).
12. Hilsenrath, J., "Tables of Thermal Properties of Gases," *Nat. Bur. Std. Cir. 564* (1955).
13. Page, F., W. H. Corcoran, W. G. Schlinger, and B. H. Sage, *Ind. Eng. Chem.*, **44**, 419 (1952).
14. Gerhart, R. V., F. C. Brunner, H. S. Mickley, B. H. Sage, and W. N. Lacey, *Mech. Eng.*, **64**, 270 (1942).
15. Reamer, H. H., and B. H. Sage, *Rev. Sci. Inst.*, **24**, 362 (1953).
16. Corcoran, W. H., F. Page, Jr., W. G. Schlinger, and B. H. Sage, *Ind. Eng. Chem.*, **44**, 410 (1952).
17. Jorissen, A. L. *Trans. Am. Soc. Mech. Eng.*, **74**, 905 (1952).
18. Walker, J. *AIChE J.*, **1**, 125 (1955).
19. Davis, L., Report No. 3-17, Jet Propulsion Laboratory, Calif. Inst. Tech., Pasadena (June, 1952).
20. Davis, L., Report No. 3-22, Jet Propulsion Laboratory, Calif. Inst. Tech., Pasadena (November, 1950).
21. Loitziansky, L. D., and B. A. Schwab, Report 329, Central Aerodynamic Hydraulic Inst., U.S.S.R. (1935).
22. Loitziansky, L. D., and B. A. Schwab, *Tech. Phys. (U.S.S.R.)*, **2**, 414 (1935).
23. Raithby, G. D., and E. R. G. Eckert, *Int. J. Heat Mass Transfer*, **11**, 1233 (1968).
24. Schnautz, J. A., Ph.D. dissertation, Oregon State College, Corvallis (1958).
25. Lavender, W. J., and D. C. T. Pei, *Int. J. Heat Mass Transfer*, **10**, 529 (1967).
26. Maisel, D. S., and T. K. Sherwood, *Chem. Eng. Prog.*, **46**, 131 (1950).
27. Galloway, T. R., and B. H. Sage, *AIChE J.*, **13**, 563 (1967).
28. Korobkin, I., A.S.M.E. Preprint 54-F-18 Rev. (1955).
29. Sibulkin, M., *J. Aero. Sci.*, **19**, 570 (1952).
30. Frössling, Nils, NACA TM 1432 (1958).

Manuscript received May 18, 1970; revision received July 27, 1971; paper accepted August 3, 1971.